Published in final edited form as:
J Hepatol. 2013 January ; 58(1): 148–154. doi:10.1016/j.jhep.2012.08.009.

Exposure to Ambient Particulate Matter Induces a NASH-like Phenotype and Impairs Hepatic Glucose Metabolism in an Animal Model

Ze Zheng[1], **Xiaohua Xu**[4], **Xuebao Zhang**[1], **Aixia Wang**[3,4], **Chunbin Zhang**[1], **Maik Hüttemann**[1], **Lawrence I. Grossman**[1], **Lung Chi Chen**[5], **Sanjay Rajagopalan**[3], **Qinghua Sun**[3,4], and **Kezhong Zhang**[1,2,*]

[1]Center for Molecular Medicine and Genetics, Wayne State University School of Medicine, Detroit, MI 48201, USA

[2]Department of Immunology and Microbiology, Wayne State University School of Medicine, Detroit, MI 48201, USA

[3]Division of Cardiovascular Medicine, Davis Heart & Lung Research Institute, College of Medicine, Ohio State University, Columbus, OH 43210, USA

[4]Division of Environmental Health Sciences, College of Public Health, Ohio State University, Columbus, OH 43210, USA

[5]Department of Environmental Medicine, New York University, Tuxedo, NY 10987, USA

Abstract

Background—Air pollution is a global challenge to public health. Epidemiological studies have linked exposure to ambient particulate matter with aerodynamic diameters < 2.5 μm ($PM_{2.5}$) to the development of metabolic diseases. In this study, we investigated the effect of $PM_{2.5}$ exposure on liver pathogenesis and the mechanism by which ambient $PM_{2.5}$ modulates hepatic pathways and glucose homeostasis.

Methods—Using "Ohio's Air Pollution Exposure System for the Interrogation of Systemic Effects (OASIS)-1", we performed whole-body exposure of mice to concentrated ambient $PM_{2.5}$ for 3 or 10 weeks. Histological analyses, metabolic studies, as well as gene expression and molecular signal transduction analyses were performed to determine the effects and mechanisms by which $PM_{2.5}$ exposure promotes liver pathogenesis.

Results—Mice exposed to $PM_{2.5}$ for 10 weeks developed a non-alcoholic steatohepatitis (NASH)-like phenotype, characterized by hepatic steatosis, inflammation, and fibrosis. Mice after $PM_{2.5}$ exposure displayed impaired hepatic glycogen storage, glucose intolerance, and insulin resistance. Further investigation revealed that exposure to $PM_{2.5}$ led to activation of inflammatory response pathways mediated through c-Jun N-terminal kinase (JNK), nuclear factor kappa B (NF-κB), and Toll-like receptor 4 (TLR4) but suppression of the insulin receptor substrate 1 (IRS1)-

*Corresponding Athour: Kezhong Zhang, Ph.D., Center for Molecular Medicine and Genetics, Wayne State University School of Medicine, 540 E. Canfield Avenue, Detroit, MI 48201, Tel: 313-577-2669; FAX: 313-577-5218; kzhang@med.wayne.edu.

mediated signaling. Moreover, $PM_{2.5}$ exposure repressed expression of the peroxisome proliferator-activated receptor (PPAR) γ and PPARα in the liver.

Conclusions—Our study suggests that $PM_{2.5}$ exposure represents a significant "hit" that triggers a NASH-like phenotype and impairs hepatic glucose metabolism. The information from this work has important implications in our understanding of air pollution-associated metabolic disorders.

Keywords

Air pollution; NASH; Glucose metabolism; Liver disease

Introduction

Recent studies have indicated that exposure to fine ambient particulate matter (aerodynamic diameter < 2.5 μm, $PM_{2.5}$) is closely associated with the pathogenesis of cardiovascular disease and metabolic syndrome [1–4]. Studies from our group and others suggested that $PM_{2.5}$-triggered systemic and pulmonary inflammation (low grade) promotes a variety of maladaptive signaling pathways that may lead to insulin resistance [1, 5, 6]. Consistent with these findings, we recently demonstrated an important interaction of $PM_{2.5}$ exposure with a high-fat diet in promoting metabolic syndrome [1, 6]. These prior studies were focused on lung or adipose pathways in mediating inflammatory responses but had not pronounced effects of $PM_{2.5}$ exposure on modulating hepatic pathways associated with metabolic disease.

Nonalcoholic fatty liver disease (NAFLD) is a spectrum of liver diseases ranging from simple non-alcoholic fatty liver (NAFL), to nonalcoholic steatohepatitis (NASH), to irreversible cirrhosis [7]. NAFLD is considered a precursor or hepatic manifestation of cardiovascular disease and metabolic syndrome. The progression of NASH is explained by a "two-hit" working model [8]. According to this model, steatosis represents the "first hit," which increases the vulnerability of the liver to various "second hits" induced by endotoxin, saturated fatty acids, inflammatory cytokines, oxidative stress, or other liver injuries. The "second hit" in turn leads to hepatic inflammation and fibrosis, the key features of NASH. Recent works showed that $PM_{2.5}$ exposure can activate Kupffer cells in murine liver tissue, which suggests that $PM_{2.5}$ may represent a risk factor for NAFLD progression [9, 10].

In this study, we used a "real-world" $PM_{2.5}$ exposure system to perform whole-body exposure of mice to environmentally relevant $PM_{2.5}$. We demonstrate that exposure to $PM_{2.5}$ causes a NASH-like phenotype and impairs hepatic glycogen storage in animals. Through both *in vivo* and *in vitro* analyses, we reveal the signaling pathways through which $PM_{2.5}$ exposure promotes NASH-associated activities and impairment of hepatic glucose metabolism.

Materials and Methods

Exposure of animals to ambient $PM_{2.5}$

Mice were exposed to concentrated ambient $PM_{2.5}$ or filtered air (FA) in a mobile trailer "Ohio's Air Pollution Exposure System for the Interrogation of Systemic Effects (OASIS)-1" in Columbus, OH, where most of the $PM_{2.5}$ components are attributed to long-range transport (Supplemental figure 1) [1]. The concentrated $PM_{2.5}$ was generated using a versatile aerosol concentration enrichment system (VACES) as described previously [1, 11]. Mice were exposed to concentrated $PM_{2.5}$ at nominal 10 × ambient concentrations for 6 hours per day, 5 days per week for a total of 3 or 10 weeks, as detailed previously [1, 9]. The control (FA) mice in the experiment were exposed to an identical protocol with the

exception of a high-efficiency particulate-air filter positioned in the inlet valve position to remove $PM_{2.5}$ particles in the filtered air stream.

For a full description of materials and methods, see Supplemental Information.

Results

Mice after inhalation exposure to $PM_{2.5}$ develop a NASH-like phenotype

To elucidate *in vivo* effects of $PM_{2.5}$ exposure, male C57BL/6 mice were exposed to concentrated ambient $PM_{2.5}$ or filtered air (FA) for 3 or 10 weeks (5 days/week, 6 hours/day) in exposure chambers of "OASIS-1", which was composed of the Midwestern regional background in Columbus, USA, where most of the $PM_{2.5}$ is attributed to long-range transport (Supplemental figure 1) [9]. It has been demonstrated that the distribution and size of concentrated $PM_{2.5}$ in the OASIS-1 exposure chamber air truly reflect that of non-concentrated $PM_{2.5}$ present in the ambient air [11, 12]. The "OASIS-1" system enables studies on animal models that recapitulate personal, short- or long-term exposure to environmentally relevant $PM_{2.5}$.

During the exposure time period, the mean daily ambient $PM_{2.5}$ concentration was 6.5μg/m^3, while the mean concentration of $PM_{2.5}$ in the exposure chamber was 74.6μg/m^3 [9]. The mice were exposed to concentrated $PM_{2.5}$ or FA for 6 hours per day, 5 days per week. After taking into account the unexposed time and weekends, the calculated average daily $PM_{2.5}$ concentration to which the mice were exposed was 11.6 μg/m^3 [the annual average $PM_{2.5}$ National Ambient Air Quality Standard is 15.0 μg/m^3 (epa.gov/air/criteria.html)]. Previously, our X-ray fluorescence spectroscopic analysis of $PM_{2.5}$ composition in the exposure chambers revealed that the major components of $PM_{2.5}$ complex are alkali metals, alkaline earth metals, transition metals, poor metals, non-metals, metalloid, and halogens [9].

To evaluate the impact of $PM_{2.5}$ exposure in liver pathology, we performed histological analyses with liver tissue sections of the mice exposed to $PM_{2.5}$ or FA for 3 or 10 weeks. Based on H&E staining of the liver cellular structure as well as Sirius-red and Masson's trichrome staining of hepatic collagen deposition, we identified hepatic steatosis, lobular and portal inflammation, and perisinusoidal fibrosis in the liver of the mice exposed to $PM_{2.5}$ for 10 weeks (Figure 1A). In comparison, the mice exposed to $PM_{2.5}$ for 3 weeks displayed non-significant, subtle hepatic steatosis, lobular inflammation, and hepatocyte ballooning (Supplemental figure 2). Using the NAFLD grading and staging score system, we confirmed that the mice exposed to $PM_{2.5}$ for 10 weeks developed modest NASH, characterized by steatosis, hepatic inflammation, and perisinusoidal fibrosis (Figure 1B).

Exposure to $PM_{2.5}$ reduces hepatic glycogen storage and impairs glucose and insulin homeostasis

To assess the impact of $PM_{2.5}$ exposure in liver metabolism, we examined glucose and insulin homeostasis in the mice exposed to $PM_{2.5}$ or FA. Under normal conditions, glycogen storage is located in the area close to central veins in the liver tissue [13]. The mice exposed to $PM_{2.5}$, but not FA, for 10 weeks lost the normal distribution of glycogen storage around central veins, as indicated by Periodic-acid Schiff (PAS) staining of glycogens in liver tissue sections (Figure 2A). Both the glycogen staining and the enzymatic assessment of hepatic glycogen indicated that levels of glycogen in the $PM_{2.5}$-exposed mouse liver were reduced, compared to that in the FA-exposed mouse liver (Figure 2A–B), suggesting a significant negative effect of $PM_{2.5}$ exposure on hepatic glycogen storage. In comparison, the amounts and distribution of hepatic glycogen in the mice exposed to $PM_{2.5}$ for 3 weeks were similar to those in the FA-exposed control mice (Supplemental figure 3A and F).

To determine whether $PM_{2.5}$ exposure can affect glucose homeostasis, we performed an intraperitoneal glucose tolerance test (IPGTT) with the animals after exposure to $PM_{2.5}$ or FA. Upon administration of glucose, the mice exposed to $PM_{2.5}$ for 10 weeks, but not 3 weeks, had higher levels of glucose remaining in the blood (Figure 2C; Supplemental figure 3G). Moreover, fasting blood glucose and insulin levels in the mice exposed to $PM_{2.5}$ for 10 weeks were much higher than those in the FA-exposed mice (Figure 2C–D). Homeostasis model assessment of insulin resistance (HOMA-IR) data indicated that the mice exposed to $PM_{2.5}$, but not FA, displayed significant insulin resistance (Figure 2E). Additionally, body weights of the mice after $PM_{2.5}$ exposure were slightly reduced, compared to that of the FA-exposed mice (Figure 2F; Supplemental figure 3H).

Exposure to $PM_{2.5}$ represses the signaling pathway mediated through the insulin receptor substrate 1 (IRS1)

We investigated potential signal transduction pathways in the liver through which $PM_{2.5}$ exposure disrupts glucose and insulin homeostasis. Glycogen synthesis is stimulated by the insulin receptor via activation of IRS1 [14]. It is known that phosphorylation of IRS1 at the residues Ser636 and/or Ser1101 inhibits IRS1-mediated insulin signaling through Akt kinase in regulating glycogen synthesis and blood glucose levels [14, 15]. Immunoblotting analysis indicated that phosphorylation of IRS1 at both Ser636 and Ser1101 was increased in the liver tissue of the mice exposed to $PM_{2.5}$, compared to that of the FA-exposed mice (Figure 2G), indicating $PM_{2.5}$-triggered inhibition of the IRS1 signaling. Consistently, phosphorylation of Akt, the downstream of IRS1 in regulating glycogen synthesis [16], was decreased in the liver of the mice exposed to $PM_{2.5}$, thus confirming the effect of $PM_{2.5}$ exposure on suppressing the IRS1-Akt signaling pathway (Supplemental figure 4A).

We assessed the effect of $PM_{2.5}$ on IRS1 signaling in hepatic stellate cells (HSC), a cell type in liver that interacts with resident macrophages to play critical roles in liver metabolism and fibrosis [17]. LX-2 is a human HSC cell line that retains the key features of HSC and has been used as an experimental tool in studying liver metabolism and fibrosis [18]. We cultured LX-2 cells in conditioned medium from the mouse macrophage cell line RAW264.7 exposed to 5 μg/ml of $PM_{2.5}$, a justified $PM_{2.5}$ concentration that can induce intracellular stress response and macrophage activation *in vitro* (Supplemental figure 5). Immunoblotting analysis showed that the phosphorylation of IRS1 at both Ser1101 and Ser636 was increased in LX-2 cells exposed to the $PM_{2.5}$-containing conditioned medium in a time-dependent manner (Supplemental figure 4B), thus confirming the suppression effect of $PM_{2.5}$ on the IRS1-mediated signaling.

$PM_{2.5}$ exposure leads to dysregulated lipid homeostasis and reduced expression of PPARγ and PPARα in the liver

We next examined the impact of $PM_{2.5}$ exposure in lipid metabolism. Consistent with the hepatic steatosis phenotype (Figure 1), accumulation of hepatic lipid droplets, as indicated by Oil-red O staining, was increased in the liver of mice exposed to $PM_{2.5}$ for 10 weeks (Figure 3A). The accumulation of hepatic lipid contents was further confirmed by the increased levels of hepatic triglycerides (TG) and cholesterol detected in the liver of the $PM_{2.5}$-exposed mice (Figure 3B–C). Moreover, levels of plasma TG and low/very low-density lipoproteins (LDL/VLDL) were elevated, while levels of plasma high-density lipoproteins (HDL) were not significantly changed in the mice exposed to $PM_{2.5}$ for 10 weeks (Figure 3D–E). However, no significant induction of liver enzymes aspartate amino transferase (AST) and alanine aminotransferase (ALT), the indicators of liver damage [19], was detected in the $PM_{2.5}$-exposed mice (Supplemental figure 6). Additionally, the mice exposed to $PM_{2.5}$ for 3 weeks only displayed marginal increase in hepatic steatosis (Supplemental figures 2 & 3A–C) and plasma TG levels (Supplemental figure 3D).

PPARs play important roles in the regulation of cellular differentiation, lipid and glucose metabolism, as well as inflammation [20]. In particular, levels of PPARγ and PPARα are inversely correlated with hepatic steatosis and glycogen storage in the progression of metabolic disease. Immunoblotting analysis showed that expression of two PPARγ isoforms, PPARγ1 and PPARγ2, were decreased in the livers of the mice exposed to $PM_{2.5}$ for 10 weeks, compared to that in the FA-exposed mice (Figure 3F). Expression of PPARα, a key regulator of fatty acid oxidation [20], was also decreased in the liver of $PM_{2.5}$-exposed mice (Figure 3F). Decreased expression of PPARα may contribute to hepatic steatosis in $PM_{2.5}$-exposed animals via down-regulation of fatty acid oxidation, an interesting question to be further investigated. Likely, down-regulation of PPARγ and PPARα, two key regulators of hepatic inflammation and metabolism, may partially account for the NASH-like phenotype observed in the $PM_{2.5}$-exposed animals.

$PM_{2.5}$ triggers the inflammatory pathways mediated through JNK, NF-κB, and TLR4

We assessed inflammatory responses in the livers of the animals exposed to $PM_{2.5}$. Immunohistochemical (IHC) staining of the macrophage activation marker F4/80 indicated that numbers of activated Kupffer cells (hepatic macrophages) and alveolar macrophages (pulmonary macrophages) were increased in the liver and lung of the mice exposed to $PM_{2.5}$ for 10 weeks, compared to those in the FA-exposed mice (Figure 4A). Expression of the mRNAs encoding pro-inflammatory cytokines IL1β, IL6, and TNFα was increased in the liver of the mice exposed to $PM_{2.5}$ (Figure 4B). $PM_{2.5}$-induced expression of the *Il1β*, *Il6*, and *Tnfα* genes was confirmed via *in vitro* experiment with RAW264.7 cells treated with $PM_{2.5}$ particles collected from the filters retrieved from OASIS-1 (Supplemental figure 7). Enzyme-linked immunosorbent assay (ELISA) indicated that plasma levels of TNFα, the major pro-inflammatory cytokine that is closely associated with NASH [21], were significantly increased in the mice exposed to $PM_{2.5}$ for 10 weeks (Figure 4C). Interestingly, although the mice exposed to $PM_{2.5}$ for 3 weeks exhibited marginal hepatic inflammation (Supplemental figure 2), plasma levels of TNFα were significantly increased in these mice (Supplemental figure 8B). Additionally, F4/80 IHC staining indicated a non-significant increase in numbers of activated alveolar macrophages in the lung of the mice after 3 weeks of $PM_{2.5}$ exposure (Supplemental figure 8D). Combining the results obtained from the mice exposed to $PM_{2.5}$ for 10 weeks, our studies suggest that systemic inflammation occurs from early on and is followed by lung and hepatic inflammation in the animals under $PM_{2.5}$ exposure.

To elucidate signal transduction pathways by which $PM_{2.5}$ stimulates expression of pro-inflammatory cytokines in the liver, we first examined JNK, a major inflammatory stress mediator that promotes pro-inflammatory cytokine expression by activating active-protein 1 (AP-1) [22]. JNK phosphorylation was increased in the liver of the mice exposed to $PM_{2.5}$ for 10 weeks (Figure 4D). Supporting the effect of $PM_{2.5}$ on JNK activation, levels of phosphorylated JNK were increased in RAW264.7 cells cultured with $PM_{2.5}$ (Supplemental figure 9A). Since AP-1 is the downstream *trans*-activator in regulating expression of pro-inflammatory cytokines under the JNK-mediated inflammatory response, we determined $PM_{2.5}$-triggered transcriptional activation of AP-1 in RAW264.7 cells. Upon $PM_{2.5}$ challenge, *trans*-activation of the AP-1 promoter, indicated by luciferase reporter analysis, was significantly increased in RAW264.7 cells (Supplemental figure 9B). Further, we tested whether JNK/AP-1 signaling is solely responsible for $PM_{2.5}$-triggered inflammation by using the JNK inhibitor SP600125 [23]. Suppression of JNK pathway in RAW264.7 macrophages by SP600125 did not significantly reduce induction of the *IL6* gene triggered by $PM_{2.5}$ (Supplemental figure 9C), suggesting that $PM_{2.5}$ may trigger other inflammatory pathways to induce production of pro-inflammatory cytokines. Indeed, we found that $PM_{2.5}$ exposure can also activate NF-κB, a key mediator of the inflammatory response, in the liver.

Activation of the NF-κB is initiated by signal-induced phosphorylation and degradation of NF-κB Inhibitor (IκB) [24]. Western blot analysis demonstrated that levels of phosphorylated IκB were increased in the liver of $PM_{2.5}$-exposed mice (Figure 4E), indicating activation of NF-κB pathway in the liver under $PM_{2.5}$ exposure. Furthermore, induction of Toll-like receptors (TLRs), the specific pattern recognition receptors that recognize structurally conserved molecules, can lead to activation of NF-κB and subsequent pro-inflammatory cytokine production [25]. Expression levels of *TLR2* and *TLR4* mRNAs were increased in the liver of mice exposed to $PM_{2.5}$ for 10 weeks (Supplemental figure 10A). Pre-treatment of the TLR4 signaling antagonist RP105 reduced expression levels of the pro-inflammatory cytokine genes *IL6* and *TNFα* in RAW264.7 cells in response to $PM_{2.5}$ challenge (Supplemental figure 10B–D) [26], thus confirming the involvement of TLR4-mediated signaling in $PM_{2.5}$-triggered macrophage inflammation.

We have previously showed that reactive oxygen species (ROS) production is required for $PM_{2.5}$-induced ER-stress response in macrophages [9]. To further delineate the mechanism underlying $PM_{2.5}$-triggered inflammation, we tested whether $PM_{2.5}$-triggered inflammation depends on intracellular ROS. ROS production from NAPDH oxidase or mitochondria in macrophages was blocked by over-expressing dominant negative N17Rac1, the small GTPase component of NADPH oxidase, or manganese superoxide dismutase (Mn-SOD) using adenovirus-based expression system [9, 27]. Upon $PM_{2.5}$ challenge, expression levels of the genes encoding pro-inflammatory cytokines IL-6 and TNFα were significantly reduced in RAW264.7 macrophages expressing dominant negative N17Rac1 or Mn-SOD (Supplemental figure 11). These results indicate that ROS produced through NAPDH oxidase or mitochondria is critical for $PM_{2.5}$-triggered inflammation.

Discussion

In this study, we demonstrate that environmentally relevant $PM_{2.5}$ exposure induces a "NASH-like" phenotype and alters glucose/insulin signaling pathways in murine liver. This work extends our prior observations on the link between air-pollution exposure and abnormalities in glucose homeostasis [1, 6]. An important finding in this study is reduction of hepatic glycogen storage upon $PM_{2.5}$ exposure (Figure 2C–E). Given the central role of hepatic glycogen storage in whole body glucose homeostasis, $PM_{2.5}$-induced glucose intolerance and insulin resistance may be a direct consequence of hepatic glycogen depletion. Our study revealed that $PM_{2.5}$ exposure suppresses the function of IRS1 in glycogen synthesis by increasing phosphorylation of IRS1 at the residues Ser636 and Ser1101, which can impair IRS1-mediated insulin signaling through Akt and subsequent glycogen synthesis in the liver (Figure 2G; Supplemental figure 4) [16]. Previously, we have demonstrated impaired insulin signaling through Akt in skeletal muscle and adipose tissues of $PM_{2.5}$-exposed mice [1, 28]. Therefore, impaired insulin signaling through IRS1-Akt in skeletal muscle, adipose tissue, and liver is likely crucial to insulin resistance and glucose intolerance observed in the mice after $PM_{2.5}$ exposure.

Our study demonstrated that exposure to $PM_{2.5}$ for 10 weeks triggers inflammation pathways mediated through JNK-AP1, NF-κB, and TLR4 in the liver (Figure 4; Supplemental figures 7–10). However, at the 3-week exposure stage, lung and liver inflammation have not been significantly elevated, although systemic inflammation, reflected by increased pro-inflammatory cytokine levels in the plasma, were evidenced (Supplemental figures 2 & 8). The organs/tissues vulnerable to $PM_{2.5}$ exposure, such as blood vessels, circulating leukocytes, and adipose tissue [1, 29], may contribute to systemic inflammation at the early stage of $PM_{2.5}$ exposure. As $PM_{2.5}$ exposure gets prolonged to 10 weeks, $PM_{2.5}$ particles are delivered to the liver to activate Kupffer cells [9, 10]. The presence of $PM_{2.5}$ in the liver may act in synergy with systemic inflammation to exacerbate

hepatic inflammation and dysregulation of lipid and glucose metabolism, an interesting question to be further investigated in the future.

The finding of $PM_{2.5}$-mediated repression of PPARγ and PPARα in the liver was quite unexpected (Figure 3F). The reduction of PPARγ is consistent with $PM_{2.5}$-mediated JNK activation (Figure 4D), which has been reported to down-regulate transcriptional activity of PPARγ [30]. In the liver, PPARα is a key regulator of fatty acid oxidation and anti-inflammatory response, while PPARγ is required to prevent inflammation and to maintain lipid and glucose homeostasis in Kupffer cells and hepatocytes [20]. Down-regulation of PPARα may be partially responsible for hepatic steatosis in $PM_{2.5}$-exposed animals due to reduction of fatty acid oxidation. Additionally, glycogen synthase, the rate-limiting enzymes for hepatic glycogen production, is a target of PPARα and PPARγ [31]. The decreased expression of hepatic PPARα and PPARγ may also contribute to the reduction of hepatic glycogen storage in $PM_{2.5}$-exposed mice (Figure 2A–B). Together, down-regulation of PPARα and PPARγ, up-regulation of inflammatory responses, and impairment of IRS1 signaling in the liver are critical to the progression of hepatic steatosis, inflammation, as well as impaired glucose and insulin homeostasis in the mice exposed to $PM_{2.5}$ for 10 weeks.

Our findings needs to be placed in the context of levels of air-pollution noted in the US. Recent epidemiologic studies have linked air pollution to the development of Type-2 diabetes [2–4]. Diabetes prevalence in the US increased with increasing $PM_{2.5}$ concentrations, as evidenced by a 1% increase in diabetes prevalence seen with a 10 $\mu g/m^3$ increase in $PM_{2.5}$ exposure [4]. The relationship remained consistent even for counties within guidelines for EPA $PM_{2.5}$ exposure limits. Interestingly, those with the highest exposure showed a >20% increase in diabetes prevalence compared with those with the lowest levels of $PM_{2.5}$, an association that persisted after controlling for diabetes risk factors [4]. In the US, 6 of the top 25 cities considered most polluted as reported by American Lung Association from 2007–2011 (www.stateoftheair.org/2011/city-rankings) are from the Midwestern region (Pittsburgh, PA; Cincinnati, OH; Cleveland, OH; Detroit, MI; Indianapolis, IN; Chicago, IL). Columbus, where our animals were exposed to $PM_{2.5}$, is a regional representative of Midwest source of air pollution in the US (Supplemental figure 1). The results from our study are consistent with maladaptive responses caused by air pollutants that may interact with other risk factors in facilitating whole body metabolic impairment. These findings significantly contribute to our understanding of air pollution-associated systemic disease, especially in the context of the burgeoning national and international epidemic of metabolic disease.

Supplementary Material

Refer to Web version on PubMed Central for supplementary material.

Acknowledgments

Portions of this work were supported by National Institutes of Health (NIH) grants DK090313 and ES017829 to KZ, American Heart Association Grants 0635423Z and 09GRNT2280479 to KZ, NIH grants ES016588, ES017412, and ES018900 to QS, and NIH grants R01ES019616, R01ES017290, and R01ES015146 to SR. We thank Dr. Scott Friedman for providing LX-2 cells and Dr. Michael Tainsky for providing AP-1 reporter plasmids.

Abbreviations

PM	ambient particulate matter
$PM_{2.5}$	PM with aerodynamic diameter less than 2.5 μm

FA	filtered air
OASIS-1	Ohio's Air Pollution Exposure System for the Interrogation of Systemic Effects
NASH	nonalcoholic steatohepatitis
HOMA-IR	homeostasis model assessment-insulin resistance
PPAR	peroxisome proliferator-activated receptor
JNK	the c-JUN N-terminal kinase
IRS1	insulin receptor substrate 1
NF-κB	Nuclear Factor-KappaB
TLRs	Toll-like receptors

References

1. Sun Q, Yue P, Deiuliis JA, Lumeng CN, Kampfrath T, Mikolaj MB, et al. Ambient Air Pollution Exaggerates Adipose Inflammation and Insulin Resistance in a Mouse Model of Diet-Induced Obesity. Circulation. 2009; 119:538–546. [PubMed: 19153269]
2. Chen JC, Schwartz J. Metabolic syndrome and inflammatory responses to long-term particulate air pollutants. Environ Health Perspect. 2008; 116:612–617. [PubMed: 18470293]
3. Kramer U, Herder C, Sugiri D, Strassburger K, Schikowski T, Ranft U, et al. Traffic-related air pollution and incident type 2 diabetes: results from the SALIA cohort study. Environ Health Perspect. 2010; 118:1273–1279. [PubMed: 20504758]
4. Pearson JF, Bachireddy C, Shyamprasad S, Goldfine AB, Brownstein JS. Association between fine particulate matter and diabetes prevalence in the US Diabetes care. 2010; 33:2196–2201.
5. Brook RD, Jerrett M, Brook JR, Bard RL, Finkelstein MM. The relationship between diabetes mellitus and traffic-related air pollution. J Occup Environ Med. 2008; 50:32–38. [PubMed: 18188079]
6. Xu X, Yavar Z, Verdin M, Ying Z, Mihai G, Kampfrath T, et al. Effect of early particulate air pollution exposure on obesity in mice: role of p47phox. Arterioscler Thromb Vasc Biol. 2010; 30:2518–2527. [PubMed: 20864666]
7. Brunt EM. Nonalcoholic steatohepatitis: definition and pathology. Semin Liver Dis. 2001; 21:3–16. [PubMed: 11296695]
8. Day CP, James OF. Steatohepatitis: a tale of two "hits"? Gastroenterology. 1998; 114:842–845. [PubMed: 9547102]
9. Laing S, Wang G, Briazova T, Zhang C, Wang A, Zheng Z, et al. Airborne particulate matter selectively activates endoplasmic reticulum stress response in the lung and liver tissues. Am J Physiol Cell Physiol. 2010; 299:C736–749. [PubMed: 20554909]
10. Tan HH, Fiel MI, Sun Q, Guo J, Gordon RE, Chen LC, et al. Kupffer cell activation by ambient air particulate matter exposure may exacerbate non-alcoholic fatty liver disease. J Immunotoxicol. 2009; 6:266–275. [PubMed: 19908945]
11. Maciejczyk P, Zhong M, Li Q, Xiong J, Nadziejko C, Chen LC. Effects of subchronic exposures to concentrated ambient particles (CAPs) in mice. II. The design of a CAPs exposure system for biometric telemetry monitoring. Inhal Toxicol. 2005; 17:189–197. [PubMed: 15804936]
12. Su Y, Sipin MF, Spencer MT, Qin X, et al. Real-Time Characterization of the Composition of Individual Particles Emitted From Ultrafine Particle Concentrators. Aerosol Sci Technol. 2006; 40:19.
13. Ulusoy E, Eren B. Histological changes of liver glycogen storage in mice caused by high-protein diets. Histol Histopathol. 2006; 21:925–930. [PubMed: 16763941]
14. Srivastava AK, Pandey SK. Potential mechanism(s) involved in the regulation of glycogen synthesis by insulin. Mol Cell Biochem. 1998; 182:135–141. [PubMed: 9609122]

15. Li Y, Soos TJ, Li X, Wu J, Degennaro M, Sun X, et al. Protein kinase C Theta inhibits insulin signaling by phosphorylating IRS1 at Ser(1101). J Biol Chem. 2004; 279:45304–45307. [PubMed: 15364919]
16. Welsh GI, Wilson C, Proud CG. GSK3: a SHAGGY frog story. Trends in cell biology. 1996; 6:274–279. [PubMed: 15157454]
17. Lanthier N, Horsmans Y, Leclercq IA. The metabolic syndrome: how it may influence hepatic stellate cell activation and hepatic fibrosis. Curr Opin Clin Nutr Metab Care. 2009; 12:404–411. [PubMed: 19474722]
18. Xu L, Hui AY, Albanis E, Arthur MJ, O'Byrne SM, Blaner WS, et al. Human hepatic stellate cell lines, LX-1 and LX-2: new tools for analysis of hepatic fibrosis. Gut. 2005; 54:142–151. [PubMed: 15591520]
19. Sorbi D, Boynton J, Lindor KD. The ratio of aspartate aminotransferase to alanine aminotransferase: potential value in differentiating nonalcoholic steatohepatitis from alcoholic liver disease. Am J Gastroenterol. 1999; 94:1018–1022. [PubMed: 10201476]
20. Feige JN, Gelman L, Michalik L, Desvergne B, Wahli W. From molecular action to physiological outputs: peroxisome proliferator-activated receptors are nuclear receptors at the crossroads of key cellular functions. Prog Lipid Res. 2006; 45:120–159. [PubMed: 16476485]
21. Fabbrini E, Sullivan S, Klein S. Obesity and nonalcoholic fatty liver disease: Biochemical, metabolic, and clinical implications. Hepatology. 2009; 51:679–689. [PubMed: 20041406]
22. Ip YT, Davis RJ. Signal transduction by the c-Jun N-terminal kinase (JNK)-from inflammation to development. Curr Opin Cell Biol. 1998; 10:205–219. [PubMed: 9561845]
23. Bennett BL, Sasaki DT, Murray BW, O'Leary EC, Sakata ST, Xu W, et al. SP600125, an anthrapyrazolone inhibitor of Jun N-terminal kinase. Proc Natl Acad Sci USA. 2001; 98:13681–13686. [PubMed: 11717429]
24. Gilmore TD. Introduction to NF-kappaB: players, pathways, perspectives. Oncogene. 2006; 25:6680–6684. [PubMed: 17072321]
25. Akira S. Toll-like receptor signaling. J Biol Chem. 2003; 278:38105–38108. [PubMed: 12893815]
26. Divanovic S, Trompette A, Atabani SF, Madan R, Golenbock DT, Visintin A, et al. Negative regulation of Toll-like receptor 4 signaling by the Toll-like receptor homolog RP105. Nat Immunol. 2005; 6:571–578. [PubMed: 15852007]
27. Chen AF, O'Brien T, Tsutsui M, Kinoshita H, Pompili VJ, Crotty TB, et al. Expression and function of recombinant endothelial nitric oxide synthase gene in canine basilar artery. Circ Res. 1997; 80:327–335. [PubMed: 9048652]
28. Xu X, Liu C, Xu Z, Tzan K, Zhong M, Wang A, et al. Long-term Exposure to Ambient Fine Particulate Pollution Induces Insulin Resistance and Mitochondrial Alteration in Adipose Tissue. Toxicol Sci. 2011; 124:88–98. [PubMed: 21873646]
29. Mills NL, Donaldson K, Hadoke PW, Boon NA, MacNee W, Cassee FR, et al. Adverse cardiovascular effects of air pollution. Nat Clin Pract Cardiovasc Med. 2009; 6:36–44. [PubMed: 19029991]
30. Camp HS, Tafuri SR, Leff T. c-Jun N-terminal kinase phosphorylates peroxisome proliferator-activated receptor-gamma1 and negatively regulates its transcriptional activity. Endocrinology. 1999; 140:392–397. [PubMed: 9886850]
31. Mandard S, Stienstra R, Escher P, Tan NS, Kim I, Gonzalez FJ, et al. Glycogen synthase 2 is a novel target gene of peroxisome proliferator-activated receptors. Cell Mol Life Sci. 2007; 64:1145–1157. [PubMed: 17437057]

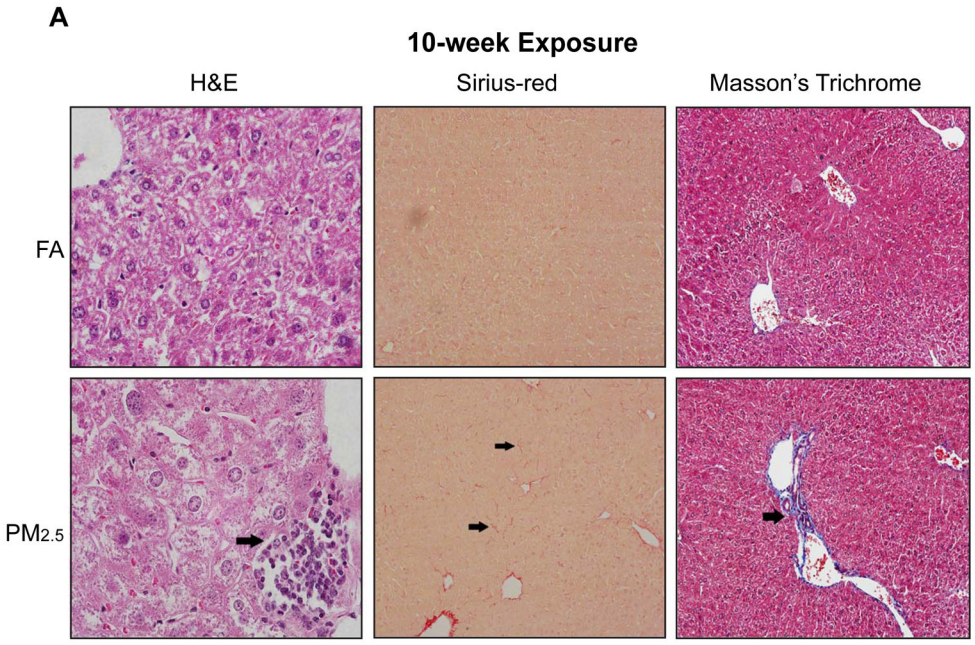

B

NAFLD grading and staging in C57BL/6J mice exposed to FA or $PM_{2.5}$

	Steatosis	Ballooning	Lobular inflammation	Portal inflammation	Mallory bodies	Grade (0-3)	Stage (0-4)
FA (4)	0.25 ± 0.25	0.00 ± 0.00	0.25 ± 0.25	0.00 ± 0.00	0.00 ± 0.00	0.25 ± 0.25	0.25 ± 0.25
$PM_{2.5}$ (5)	1.2 ± 0.20	0.60 ± 0.40	0.80 ± 0.20	0.40 ± 0.24	0.20 ± 0.20	1.6 ± 0.24	1.40 ± 0.24
P-value	0.024	0.208	0.135	0.178	0.374	0.007	0.014

Number of mice examined is given in parenthese. Mean ± SEM values are shown. P-values were calculated by Mann-Whitney U-test

Figure 1. $PM_{2.5}$ exposure induces a NASH-like phenotype in mouse liver

(**A**) Histological analysis of liver cellular structure (H&E staining, 600×), collagen deposition (Sirius-red staining, 200×), and collagen fiber (Masson's Trichrome Staining, 600×) in liver tissue sections from mice exposed to FA or $PM_{2.5}$ for 10 weeks. The arrows point out areas of hepatic inflammation or fibrosis. (**B**) Histological scoring for NASH activities in the livers of mice exposed to $PM_{2.5}$ or FA for 10 weeks. The Grade scores were calculated based on the scores of steatosis, hepatocyte ballooning, lobular and portal inflammation, and Mallory bodies. The Stage scores were based on liver fibrosis. Mean ± SEM values are shown (n=4 mice for FA-exposed group or 5 mice for $PM_{2.5}$-exposed group).

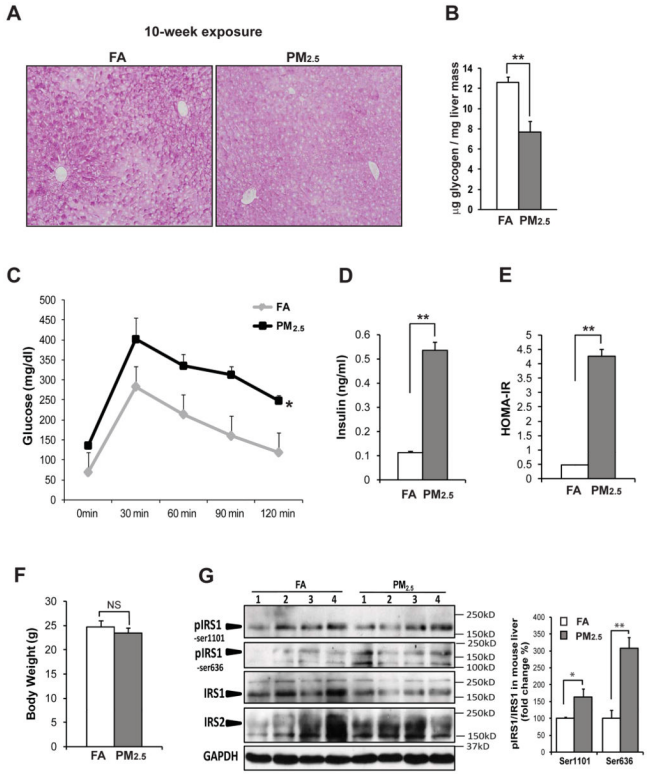

Figure 2. Exposure to $PM_{2.5}$ leads to impaired hepatic glycogen storage, glucose intolerance, and insulin resistance

(**A**) Periodic-acid Schiff's staining of hepatic glycogens in the livers of mice exposed to $PM_{2.5}$ or FA for 10 weeks (magnification: 200×). (**B**) Levels of hepatic glycogens in the liver tissues of the mice exposed to $PM_{2.5}$ or FA for 10 weeks. (**C**) IPGTT analysis with the mice exposed to $PM_{2.5}$ or FA for 68 days. Blood glucose levels were measured after i.p. injection of 2mg glucose/gram body weight into the animals fasted for 12 hours. Measurement of fast blood glucose and insulin levels as well as IPGTT analysis were performed 2 days ahead of animal euthanization. (**D**) Fast blood insulin levels in mice exposed to $PM_{2.5}$ or FA. Blood insulin levels were determined with the mice after 12 hours of fasting. (**E**) Homeostasis Model of Assessment of Insulin Resistance (HOMA-IR) for the mice exposed to $PM_{2.5}$ or FA. (**F**) Body weights of mice exposed to $PM_{2.5}$ or FA for 10 weeks. (**G**) Immunoblotting analysis of phosphorylated and total IRS1 as well as IRS2 in the liver tissues of the mice exposed to $PM_{2.5}$ or FA. The graph shows fold changes of the ratios of phosphorylated *vs* total IRS1 in liver tissues. For panels B–G, each bar or point denotes mean ± SEM (n= 4 mice). * $p<0.05$; ** $p<0.01$; NS, non-significant.

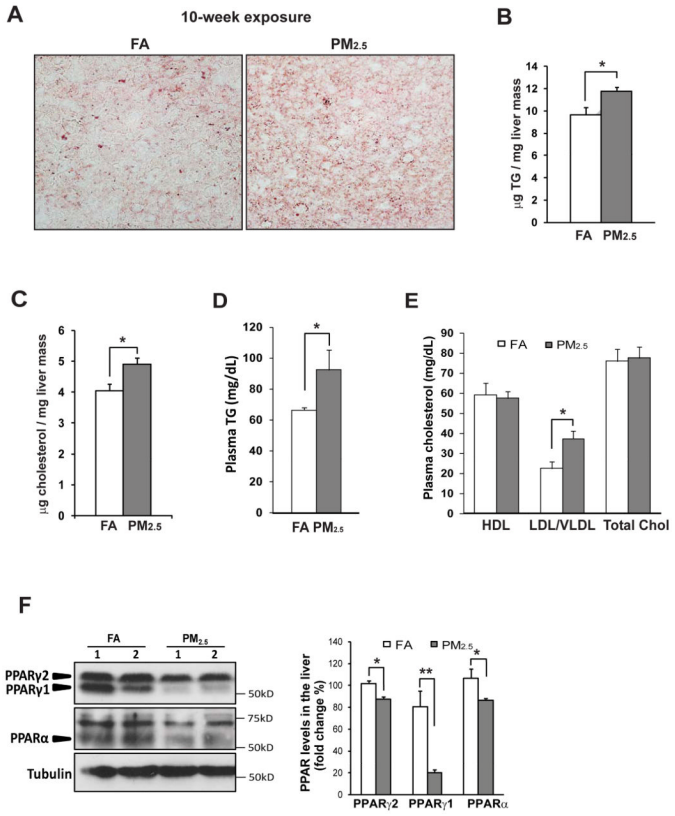

Figure 3. $PM_{2.5}$ exposure leads to hepatic steatosisand down-regulates expression of PPARs

(A) Oil-red O staining of lipid droplets in the livers of the mice exposed to $PM_{2.5}$ or FA for 10 weeks (magnification: 600×). (**B–E**) Levels of hepatic TG (B), hepatic cholesterol (C), plasma TG (D), and plasma cholesterol (E) of the mice exposed to $PM_{2.5}$ or FA for 10 weeks. Total chol, total plasma cholesterol. (**F**) Immunoblotting analysis of PPARγ and PPARα in the liver tissue from the mice exposed to $PM_{2.5}$ or FA for 10 weeks. The graph beside the images shows fold changes of PPARγ1, PPARγ2, and PPARα levels in the liver of the $PM_{2.5}$- or FA-exposed mice. For panels B–F, each bar or point denotes mean ± SEM (n= 4 mice). * $p<0.05$; ** $p<0.01$.

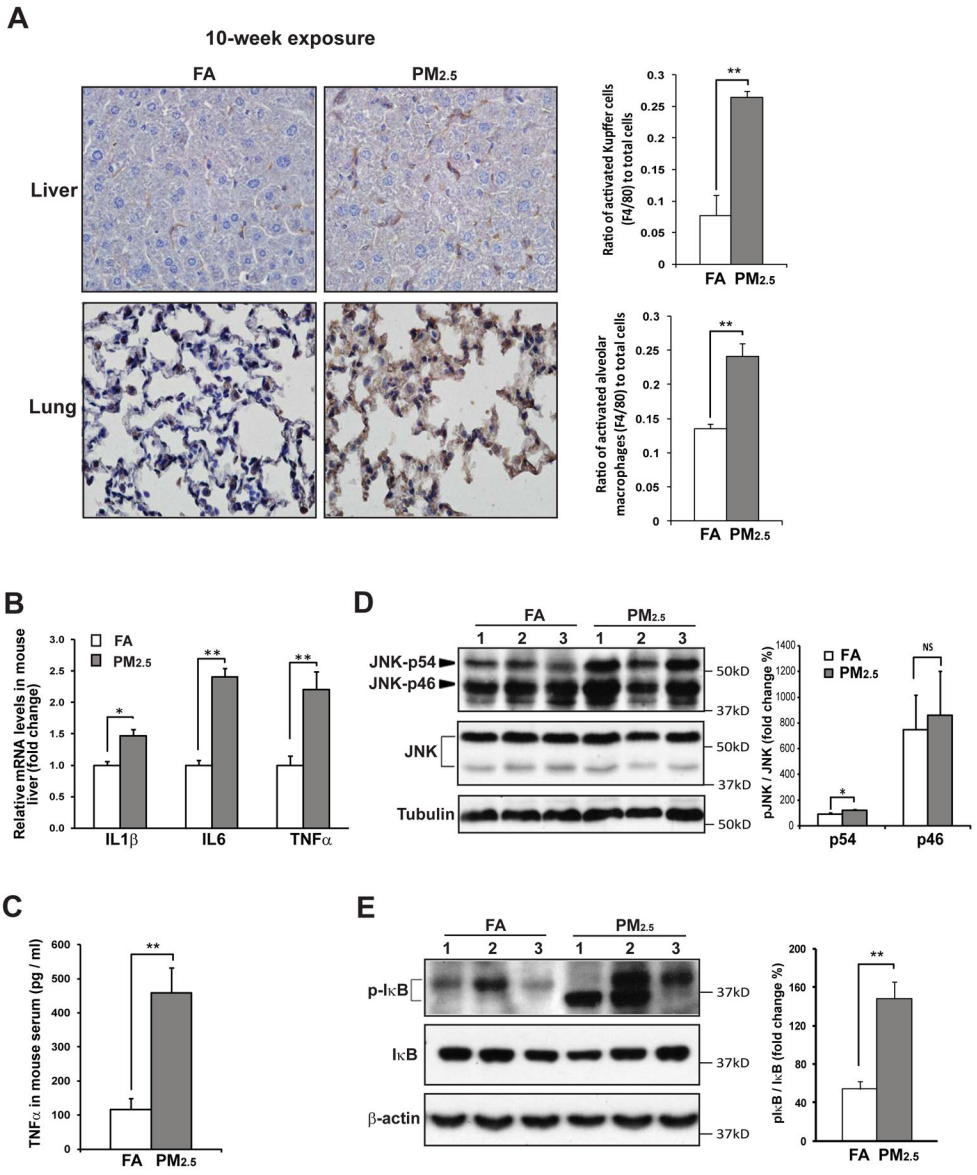

Figure 4. Exposure to $PM_{2.5}$ activates the inflammatory pathways mediated through JNK and NF-κB in the liver

(A) Immunohistochemical staining of macrophage cell surface marker F4/80 in the liver and lung tissues of the mice exposed to $PM_{2.5}$ or FA for 10 weeks (Magnification: 600×). The graph beside the image showed the ratios of F4/80-positive Kupffer cells or alveolar cells to total liver or lung cells. The ratios were determined by counting the F4/80-positive and total cells in 3 random fields per sample. Data are shown as mean ± SEM (n=3 mice per group). *** P*< 0.01. (**B**) Quantitative real-time RT-PCR analysis of the mRNAs encoding IL-1β, IL-6, and TNFα in the liver of the mice exposed to $PM_{2.5}$ or FA for 10 weeks. Fold changes of mRNA levels were determined after normalization to internal control β-actin RNA levels. Each bar denotes mean ± SEM (n= 5 mice). * $p<0.05$; ** $p<0.01$. (**C**) Plasma levels of TNFα, determined by ELISA, in the mice exposed to $PM_{2.5}$ or FA for 10 weeks (n=4 mice for FA or 5 mice for $PM_{2.5}$ group). (**D–E**) Immunoblotting analysis of phosphorylated and total JNK (D) and IκB (E) in the liver of the mice exposed to $PM_{2.5}$ or FA for 10 weeks. Levels of tubulin or β-actin were determined as loading controls. The graphs beside the

images show fold changes of the ratios of phosphorylated *vs* total JNK or IκB in the liver of $PM_{2.5}$- or FA-exposed mice (n=3 mice).